

All-optical measurement of Rashba coefficient in quantum wells

P. S. Eldridge,¹ W. J. H. Leyland,² P. G. Lagoudakis,¹ O. Z. Karimov,¹ M. Henini,³ D. Taylor,³
R. T. Phillips,² and R. T. Harley¹

¹*School of Physics and Astronomy, University of Southampton, Southampton SO17 1BJ, United Kingdom*

²*Cavendish Laboratory, Madingley Road, Cambridge CB3 0HE, United Kingdom*

³*School of Physics and Astronomy, University of Nottingham, Nottingham NG7 4RD, United Kingdom*

(Received 5 February 2008; published 31 March 2008)

We perform an all-optical spin-dynamic measurement of the Rashba spin-orbit interaction in (110)-oriented GaAs/AlGaAs quantum wells under applied electric field. This crystallographic orientation allows us to isolate the Rashba from other contributions, giving precise values of the Rashba coefficient. At low temperature, we find good agreement between our measurements and the $k \cdot p$ theory. Unexpectedly, we observe a temperature dependence of the Rashba coefficient that may signify the importance of higher-order terms of the Rashba coupling.

DOI: [10.1103/PhysRevB.77.125344](https://doi.org/10.1103/PhysRevB.77.125344)

PACS number(s): 72.25.Fe, 72.25.Rb, 73.21.Fg

I. INTRODUCTION

Semiconductor spintronic and spin-optronic quantum devices in which electronic spin orientation replaces charge for data processing or is used to control optical polarization are at the focus of intense investigations. As manipulation of electron spins has been signposted as the preferred route to quantum computing,¹ progress toward realistic devices depends on engineering the spin-orbit interactions that result in effective magnetic fields seen by the electrons as they propagate and which lead to spin precession, reorientation, and relaxation. A classic example is the Datta and Das spin transistor, wherein the precession of spin polarized electrons confined in a plane is controlled by a gate voltage which tunes the spin-orbit coupling.² Whereas the ability to tune the coupling strength originates in the field-induced spin splitting of the electronic bands, known as the Rashba [or structural inversion asymmetry (SIA)] effect, other contributions to the spin splitting, from bulk inversion asymmetry (BIA) (or Dresselhaus coupling) and natural interface asymmetry (NIA) in heterostructures, complicate direct characterization of the Rashba term and numerous investigations have tried to estimate the strength of these terms.³⁻⁶ Disentangling and evaluating the contributions of the different spin-orbit coupling mechanisms to the spin splitting of the electronic bands are important for the engineering of spintronic devices.

Several experimental techniques have been employed to characterize the different contributions to the spin splitting of the electronic bands. Weak antilocalization analysis was used as a function of the structural inversion asymmetry in InAlAs/InGaAs quantum wells (QWs) to derive values of the Rashba spin-orbit coupling constant, although neglecting the contribution of the Dresselhaus term,³ whereas the relative strength of the Rashba and Dresselhaus terms was accurately estimated from photocurrent measurements on n -type InAs QWs containing a two-dimensional electron gas (2DEG) by utilizing the angular distribution of the spin-galvanic effect in the plane of the QW.⁴ In a different configuration, GaAs/AlGaAs 2DEG heterostructures were grown to study the transition from weak localization to weak antilocalization, and using magnetoconductance measure-

ments, the spin-orbit magnetic field was calculated as a function of electron density, from which the Rashba term and the linear and cubic Dresselhaus terms were derived.⁵ Here, we have designed and grown (110)-oriented GaAs/AlGaAs quantum well heterostructures in which the crystallographic orientation of the quantum confinement allows separation of the terms. Through combined optical measurements of spin relaxation in applied electric field and of electron drift mobility, we measure the spin splitting as a function of applied field and so derive the Rashba coefficient. The spin-relaxation rates are derived from optical Kerr-rotation measurements⁷ and the drift mobility is measured using the spin-grating technique developed in Ref. 8.

The spin-orbit interaction can be represented as an electron spin precession vector $\mathbf{\Omega}(\mathbf{k})$ which is the sum of the three components described above, denoted $\mathbf{\Omega}^{\text{SIA}}(\mathbf{k})$, $\mathbf{\Omega}^{\text{BIA}}(\mathbf{k})$, and $\mathbf{\Omega}^{\text{NIA}}(\mathbf{k})$,^{1,9} where \mathbf{k} is the electron wave vector. For a symmetrical quantum well, to first order, the SIA term has the form^{9,10}

$$\mathbf{\Omega}^{\text{SIA}}(\mathbf{k}) = \alpha(e/\hbar)\mathbf{F} \times \mathbf{k}, \quad (1)$$

where α is the Rashba coefficient and \mathbf{F} the electric field. For field applied along the growth axis, $\mathbf{\Omega}^{\text{SIA}}(\mathbf{k})$ lies in the quantum well plane because \mathbf{k} is confined to the plane. If the growth plane is (110), the electron motion is confined to the (110) plane, and it can be shown that $\mathbf{\Omega}^{\text{BIA}}(\mathbf{k})$ is, by symmetry, normal to the plane, parallel or antiparallel to the growth axis [110].^{1,11} In the case of (110)-oriented growth, the NIA component is zero because the interfaces contain equal numbers of anions and cations.^{1,12} Thus, for electric field applied along the growth axis, $\mathbf{\Omega}(\mathbf{k})$ has just two components, $\mathbf{\Omega}^{\text{SIA}}(\mathbf{k})$ and $\mathbf{\Omega}^{\text{BIA}}(\mathbf{k})$, which are orthogonal for all electron wave vectors.

The spin relaxation of a nonequilibrium population of electron spins in noncentrosymmetric semiconductors may involve several mechanisms.¹ In quantum wells, the dominant one in all except p -type material is that identified by D'yakonov *et al.*^{11,13} where the spin precession due to spin-orbit interaction is the driving force for spin reorientation, and therefore loss of spin memory. Strong scattering of the electron wave vector randomizes the precession and causes

spin relaxation. The relaxation rate for the component of a spin population along a particular axis, i , is given by¹

$$\tau_{s,i}^{-1} = \langle \Omega_{\perp}^2 \rangle \tau_p^* \quad (\langle |\Omega| \rangle \tau_p^* \ll 1), \quad (2)$$

where $\langle \Omega_{\perp}^2 \rangle$ is the averaged square component of $\Omega(\mathbf{k})$ in the plane *perpendicular* to the axis i taken over the spin-oriented population and τ_p^* is the momentum scattering time of an electron. Thus, in a (110)-oriented quantum well with electric field applied along the growth axis, relaxation of the in-plane components of spin involves both Ω^{BIA} and Ω^{SIA} but the relaxation of the growth-axis component is determined by Ω^{SIA} alone. Here, we use measurements of spin relaxation along the growth axis in applied electric field to determine directly the Rashba (SIA) coefficient α .

Squaring Eq. (1) and taking the thermal average assuming $k_B T \gg \hbar \Omega^{\text{SIA}}$ gives

$$\langle (\Omega^{\text{SIA}})^2 \rangle = \alpha^2 \frac{e^2}{\hbar^2} F^2 \langle k^2 \rangle = \alpha^2 \frac{e^2}{\hbar^2} F^2 \frac{2m^* k_B T}{\hbar^2}, \quad (3)$$

where k is the in-plane component of the wave vector, m^* is the electron effective mass, and k_B is Boltzmann's constant. Substitution of Eq. (3) into Eq. (2) shows that the spin-relaxation rate along the growth axis should be linear in $F^2 \tau_p^*$ and the Rashba coefficient is given by

$$\alpha = \frac{\hbar^2}{eF} (2m^* k_B T \tau_s \tau_p^*)^{-1/2}. \quad (4)$$

Thus, we can obtain the Rashba coefficient α from combined measurements of momentum relaxation time and of spin relaxation in applied electric field.

II. EXPERIMENTAL METHODS AND RESULTS

Our sample consisted of a GaAs/Al_{0.4}Ga_{0.6}As p^+i-n^+ structure grown on a semi-insulating (110)-oriented GaAs substrate. The insulating portion of the structure comprised 100 nm layers of undoped AlGaAs on each side of a stack of twenty 7.5 nm undoped GaAs quantum wells with 12 nm undoped AlGaAs barriers. For our pump-probe measurements of the spin-relaxation time τ_s (see below), a portion of the wafer was processed into a circular mesa device 400 μm in diameter with an annular metal contact to the top n^+ layer to allow optical access to the quantum wells and a second contact to the lower p^+ layer. The electric field was varied by means of applied bias voltage. The total electric field \mathbf{F} was obtained as the sum of that due to the external bias and that to the built-in electric field of the $p-i-n$ structure. In calculating the built-in field, we made allowance for temperature dependence of the band gap in the structure; the variation is small over the range of our measurements, values being $2.85 \times 10^6 \text{ V m}^{-1}$ at 80 K and $2.76 \times 10^6 \text{ V m}^{-1}$ at 230 K. The externally applied component was given by the ratio of applied voltage bias to width of the insulating region. All measurements were made at temperatures above 80 K in order to reveal effects of free electrons rather than excitons in the quantum wells.¹⁴

Photocurrent measurements in the $p-i-n$ device as a function of applied bias and of photon energy were used to in-

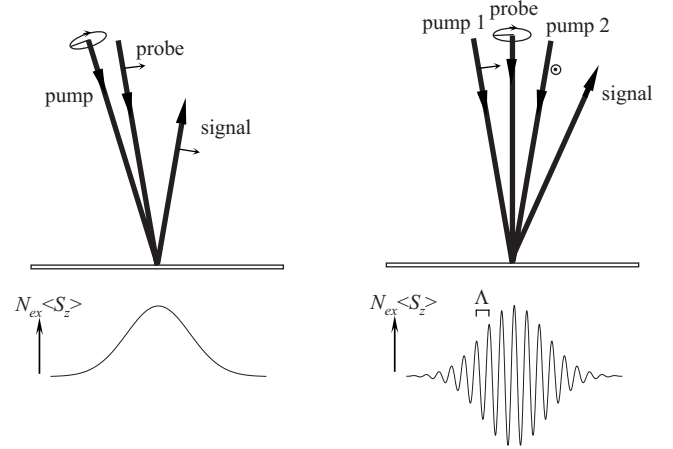


FIG. 1. Experimental configurations for measurements of (a) spin relaxation and (b) spin diffusion. Upper diagrams: incident pump and probe beams and their polarizations; lower diagrams: profile of focused pump spot with a (a) spin polarized population and (b) spin grating with spacing Λ .

vestigate the motion of the photoexcited carriers in the structure. We found that for applied reverse bias less than 3 V, the photocurrent was extremely low, indicating that the electrons, resonantly excited into the $n=1$ confined state of a quantum well, can be considered to remain there until recombination, escape processes such as thermal excitation over the barriers and phonon-assisted tunneling being negligible.¹⁵ Above 3 V there was evidence of resonant tunneling between $n=1$ and $n=2$ confined electron states in adjacent wells and of avalanche multiplication. In the measurements reported here, we therefore concentrate on applied bias less than 3 V, equivalent to $\mathbf{F} \leq 8 \times 10^6 \text{ V m}^{-1}$.

The momentum relaxation time τ_p^* was obtained as a function of temperature from measurement of the electron diffusion coefficient using a transient spin-grating method (see below) on an unprocessed portion of the same wafer. This gave τ_p^* at one value of transverse field, namely, the built-in field, $\sim 2.80 \times 10^6 \text{ V m}^{-1}$. We do not expect τ_p^* to show any significant dependence on the field and we have assumed this in our analysis. The assumption is supported by measurements in a wafer with nominally identical quantum wells but not grown in a $p-i-n$ structure so that the electric field is zero; the values of τ_p^* were the same, within experimental uncertainty, as for the $p-i-n$ structure over the temperature range investigated.

The spin relaxation of the electrons was investigated using a picosecond-resolution polarized pump-probe reflection technique [see Fig. 1(a)].⁷ Wavelength-degenerate circularly polarized pump and delayed linearly polarized probe pulses from a mode-locked Ti-sapphire laser were focused at close to normal incidence on the sample and tuned to the $n=1$ heavy-hole to conduction band transition. The pulse duration was $\sim 1.5 \text{ ps}$ and repetition frequency was 75 MHz. Absorption of each pump pulse generated a photoexcited population of electrons spin polarized along the growth axis (z). The time evolution of the photoexcited population and of the spin polarization $\langle S_z \rangle(t)$ were monitored by measuring

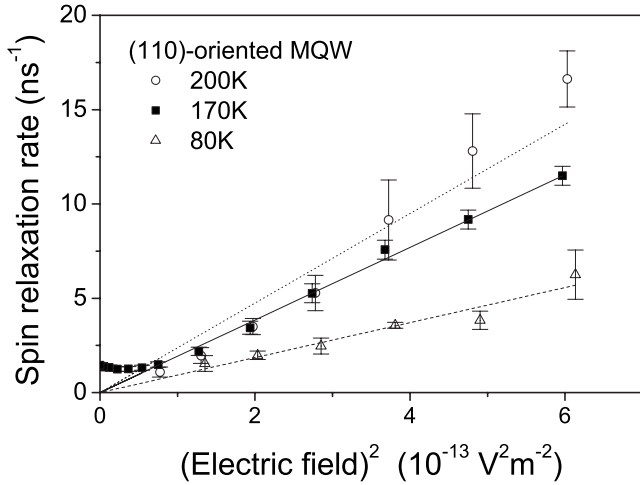


FIG. 2. Electric field dependence of spin-relaxation rate at three temperatures. The high field linear regions of the graphs extrapolate to the origin and the slopes are used to determine the Rashba coefficient.

pump-induced changes of, respectively, probe reflection ΔR and probe polarization rotation $\Delta\theta$ as functions of probe pulse delay. These measurements were combined to give the spin-relaxation rate $1/\tau_s$. They also showed that the recombination time of photoexcited carriers, τ_r , was typically five times longer than τ_s . The pump beam intensity was typically 0.5 mW focused to a 60 μm diameter spot giving an estimated photoexcited spin-polarized electron density $N_{ex} \sim 10^9 \text{ cm}^{-2}$; the probe intensity was 25% of the pump.

Figure 2 shows $1/\tau_s$ vs F^2 for three different temperatures. For fields above $\sim 3 \times 10^6 \text{ V m}^{-1}$, the relationship is linear within experimental uncertainty, demonstrating the dominance in this range of the D'yakonov-Perel'-Kachorovskii (DPK) spin-relaxation mechanism with spin splitting determined by the Rashba (SIA) effect. For lower values of field, $1/\tau_s$ tends to a constant value, indicating a changeover possibly to an alternative form of the DPK mechanism, for example, due to spin splitting associated with imperfections of the interfaces¹⁵ or to a different mechanism, possibly Bir-Aronov-Pikus spin relaxation,¹ due to accumulation of photoexcited holes under forward bias of the p - i - n structure. The lines in Fig. 2 represent best fits to the experimental points from which the Rashba coefficient is obtained.

The spin-grating measurements [see Fig. 1(b)]^{8,16} were made using twin 0.5 mW pump beams from a 200 fs pulse-length mode-locked Ti-sapphire laser tuned to the $n=1$ valence-conduction band transition. The beams were linearly polarized at 90° to one another and incident on the sample at $\pm 4.1^\circ$ to the normal. This produced interference fringes of polarization but not intensity, resulting in a transient grating of spin population with a pitch $\Lambda \sim 5.7 \mu\text{m}$. The focal spot size on the sample was again of order of 60 μm , giving excitation density $N_{ex} \sim 10^9 \text{ cm}^{-2}$. The decay rate of the amplitude of such a grating is given by⁸

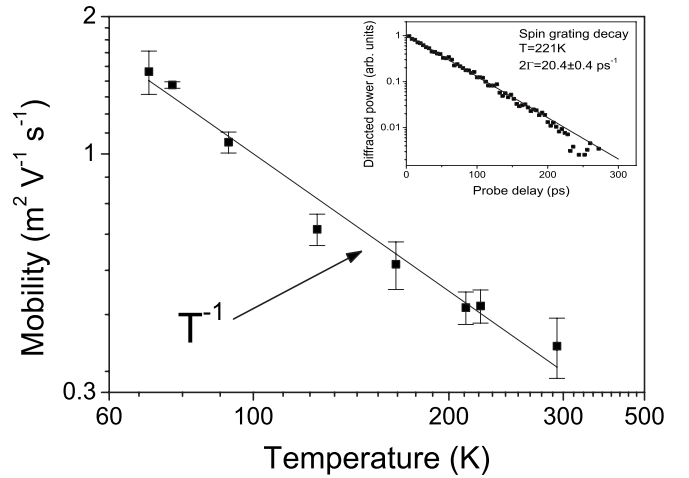


FIG. 3. Logarithmic plot of the electron mobility in a sample from the same wafer as data of Fig. 2, determined by the spin-grating method. The electric field is the built-in field of the p - i - n structure, $2.80 \times 10^6 \text{ V m}^{-1}$. The T^{-1} temperature dependence is as expected for a nondegenerate two-dimensional electron system with dominant phonon scattering. The inset is a typical grating decay signal at 221 K.

$$\Gamma = D_s \frac{4\pi^2}{\Lambda^2} + \tau_s^{-1} + \tau_r^{-1}, \quad (5)$$

where D_s is the electron spin-diffusion coefficient. The decay was monitored by measuring first-order diffraction in reflection geometry using a delayed 0.25 mW linear polarized probe beam from the same laser, incident on the sample at normal incidence. Signal to noise ratio was enhanced using an optical heterodyne detection scheme;¹⁶ in this configuration, the decay rate of the diffracted intensity is 2Γ . Since the sample was undoped, we can equate the electron spin-diffusion coefficient to the diffusion coefficient D_e and obtain the electron mobility from the Einstein equation $\mu = (e/k_B T) D_e$.

Figure 3 shows an example of a measured decay together with the extracted values of electron mobility as a function of temperature. The grating decay rate (and therefore D_e) is found to be insensitive to temperature so that $\mu \sim T^{-1}$. This temperature dependence is as expected for a nondegenerate two-dimensional electron system, that is, with constant density of states, and dominant phonon scattering with probability $\sim k_B T$.¹⁷ From the mobility, we obtain the ensemble momentum relaxation time $\tau_p = m^* \mu / e$ and since we are dealing with intrinsic material with negligible electron-electron scattering, we can equate this to the momentum scattering time τ_p^* .^{1,18}

III. DISCUSSION AND CONCLUSIONS

Figure 4 shows the values of the Rashba coefficient obtained by combining the two sets of measurements using Eq. (4). The value is approximately 0.1 nm^2 ; however, there is a clear upward trend which is consistent with a linear increase of the Rashba coefficient with electron kinetic energy. The

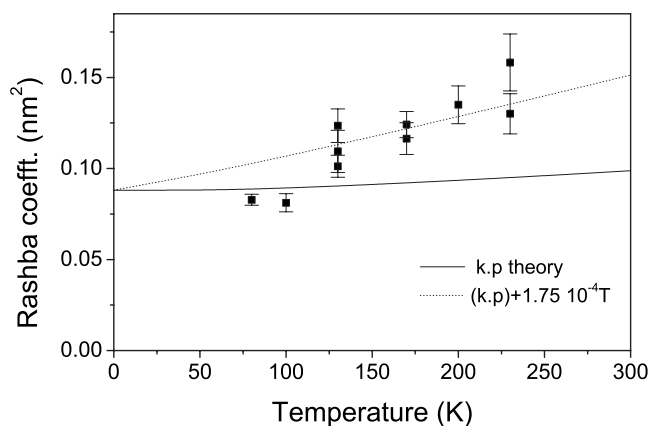


FIG. 4. Rashba coefficient obtained from combination of spin relaxation and mobility measurements. The solid curve is eight-band $k\cdot p$ calculation including temperature dependence of band edges and of interband momentum matrix element. The dotted curve is the $k\cdot p$ theory plus an empirical linear-in- T term.

solid curve is based on the eight-band $k\cdot p$ treatment given by Winkler.¹⁰ The spin splitting is given as

$$|\Omega^{\text{SIA}}| = \alpha \frac{e}{\hbar} |k| F = \frac{e^2 P^2}{3\hbar^2} \left(\frac{1}{E_g^2} - \frac{1}{(E_g + \Delta_0)^2} \right) |k| F_v, \quad (6)$$

where E_g is the band gap of GaAs, Δ_0 is the spin-orbit splitting in the valence band, and P is Kane's momentum matrix element.¹⁹ F_v is the effective electric field in the *valence band* and is given by¹⁰

$$F_v = F \left(1 + \frac{\Sigma_v}{\Sigma_c} \right) \approx 1.67F, \quad (7)$$

Σ_v and Σ_c being the valence and conduction band offsets between GaAs and AlGaAs which we take to be in the ratio of 3:2. The weak temperature dependence of the curve results from the temperature dependence of E_g combined with the recently identified temperature dependence of P .²⁰ This theoretical estimate is in satisfactory agreement with the experimental values of the Rashba coefficient, particularly at low temperature, but it does not reproduce the observed tem-

perature dependence. We note that extension of the $k\cdot p$ treatment to 14 bands, following Refs. 10 and 21, increases the calculated values by less than 2% and does not significantly change the temperature dependence. Similarly, a full quantum well calculation,¹⁰ which would involve many band parameters, will change the calculated value slightly but will not alter the temperature dependence. Thus, a theoretical understanding of the observed temperature dependence is, at present, missing.

To indicate a possible theoretical interpretation, the dotted curve in Fig. 4 is the $k\cdot p$ theory plus an empirical term linear in temperature. Within the experimental uncertainties, this reproduces the data reasonably well. As the photoexcited electron gas is nondegenerate, the additional linear temperature dependence suggests that the Rashba coefficient has an additional approximately linear dependence on the electrons' kinetic energy. This is reminiscent of the dependence of the Zeeman splitting on kinetic energy²² which, in turn, gives rise to the observed increase of the effective electron g factor with quantum confinement in GaAs/AlGaAs quantum wells.²³ The observed dependence may therefore signify the importance of the usually neglected higher-order terms in the Rashba Hamiltonian.²⁴

In conclusion, by combined measurements of spin relaxation and of electron mobility in undoped and nominally inversion symmetric (110)-oriented quantum wells in a p - i - n structure, we have been able to investigate directly the electric field spin splitting of the conduction band without interfering effects from bulk inversion or natural interface asymmetry and derive the Rashba coefficient. The observed splitting is in qualitative agreement with a theoretical $k\cdot p$ calculation¹⁰ but also reveals an unexpected temperature dependence. Direct measurement of the Rashba coefficient is important for developing an understanding of the fundamental interactions in semiconductor nanostructures and for the engineering of spintronic devices.

ACKNOWLEDGMENTS

We acknowledge useful discussions with Roland Winkler and Xavier Cartoixa and financial support of the Engineering and Physical Sciences Research Council (EPSRC).

¹For reviews, see *Optical Orientation: Modern Problems in Condensed Matter Physics* (Vol. 8), edited by F. Meier and B. P. Zakharchenya (North-Holland, Amsterdam, 1984); *Semiconductor Spintronics and Quantum Computation*, edited by D. D. Awschalom, D. Loss, and N. Samarth (Springer, Berlin, 2002); M. E. Flatté, J. M. Byers, and W. H. Lau, *ibid.* Chap. 4.

²S. Datta and B. Das, *Appl. Phys. Lett.* **56**, 665 (1990).

³T. Koga, J. Nitta, T. Akazaki, and H. Takayanagi, *Phys. Rev. Lett.* **89**, 046801 (2002).

⁴S. D. Ganichev, V. V. Bel'kov, L. E. Golub, E. L. Ivchenko, Petra Schneider, S. Giglberger, J. Eroms, J. De Boeck, G. Borghs, W. Wegscheider, D. Weiss, and W. Prettl, *Phys. Rev. Lett.* **92**, 256601 (2004); S. Giglberger, L. E. Golub, V. V. Bel'kov, S. N. Danilov, D. Schuh, C. Gerl, F. Rohlfling, J. Stahl, W. Wegscheider, D. Weiss, W. Prettl, and S. D. Ganichev, *Phys.*

Rev. B **75**, 035327 (2007).

⁵J. B. Miller, D. M. Zumbühl, C. M. Marcus, Y. B. Lyanda-Geller, D. Goldhaber-Gordon, K. Campman, and A. C. Gossard, *Phys. Rev. Lett.* **90**, 076807 (2003).

⁶L. Meier, G. Salis, I. Shorubalko, E. Gini, S. Schön, and K. Ensslin, *Nat. Phys.* **3**, 650 (2007).

⁷R. T. Harley, O. Z. Karimov, and M. Henini, *J. Phys. D* **36**, 2198 (2003).

⁸A. R. Cameron, P. Riblet, and A. Miller, *Phys. Rev. Lett.* **76**, 4793 (1996).

⁹E. L. Ivchenko, *Optical Spectroscopy of Semiconductor Nanostructures* (Alpha Science, Harrow, UK, 2005).

¹⁰R. Winkler, *Physica E (Amsterdam)* **22**, 450 (2004); R. Winkler, *Spin-Orbit Coupling Effects in Two-Dimensional Electron and Hole Systems* (Springer, New York, 2003).

- ¹¹M. I. D'yakonov and V. Yu. Kachorovskii, *Sov. Phys. Semicond.* **20**, 110 (1986).
- ¹²K. C. Hall, K. Gündoğdu, E. Altunkaya, W. H. Lau, M. E. Flatté, T. F. Boggess, J. J. Zinck, W. B. Barvosa-Carter, and S. L. Skeith, *Phys. Rev. B* **68**, 115311 (2003).
- ¹³M. I. D'yakonov and V. I. Perel', *Sov. Phys. JETP* **33**, 1053 (1971).
- ¹⁴A. Malinowski, R. S. Britton, T. Grevatt, R. T. Harley, D. A. Ritchie, and M. Y. Simmons, *Phys. Rev. B* **62**, 13034 (2000).
- ¹⁵O. Z. Karimov, G. H. John, R. T. Harley, W. H. Lau, M. E. Flatté, M. Henini, and R. Airey, *Phys. Rev. Lett.* **91**, 246601 (2003).
- ¹⁶W. J. H. Leyland, Ph.D. thesis, Cambridge University, UK, 2007.
- ¹⁷J. M. Ziman, *Electrons and Phonons* (Oxford University Press, New York, 1972), Chap. 10.
- ¹⁸W. J. H. Leyland, G. H. John, R. T. Harley, M. M. Glazov, E. L. Ivchenko, D. A. Ritchie, I. Farrer, A. J. Shields, and M. Henini, *Phys. Rev. B* **75**, 165309 (2007) and references therein.
- ¹⁹E. O. Kane, *J. Phys. Chem. Solids* **1**, 249 (1957).
- ²⁰J. Hubner, S. Dohrmann, D. Hagele, and M. Oestrich, arXiv:cond-mat/0608534 (2006).
- ²¹W. Knap, C. Skierbiszewski, A. Zduniak, E. Litwin-Staszewska, D. Bertho, F. Kobbi, J. L. Robert, G. E. Pikus, F. G. Pikus, S. V. Iordanskii, V. Mosser, K. Zekentes, and Yu. B. Lyanda-Geller, *Phys. Rev. B* **53**, 3912 (1996).
- ²²M. A. Hopkins, R. J. Nicholas, P. Pfeffer, W. Zawadzki, D. Gauthier, J. C. Portal, and M. A. DiForte-Poisson, *Semicond. Sci. Technol.* **2**, 568 (1987).
- ²³M. J. Snelling, G. P. Flinn, A. S. Plaut, R. T. Harley, A. C. Tropper, R. Eccleston, and C. C. Phillips, *Phys. Rev. B* **44**, 11345 (1991).
- ²⁴X. Cartoixà, L.-W. Wang, D. Z.-Y. Ting, and Y.-C. Chang, *Phys. Rev. B* **73**, 205341 (2006).